A&A 395, L9–L12 (2002)
DOI: 10.1051/0004-6361:20021421

Astronomy & Astrophysics

Near infrared coronagraph images of IRC +10216

Faint structures at 1–5″ from the central star

K. Murakawa[1,⋆], M. Tamura[2], H. Suto[3], Y. Itoh[3], S. S. Hayashi[3], Y. Oasa[4], Y. Nakajima[5], N. Kaifu[2], J. A. Yates[1], T. M. Gledhill[1], A. M. S. Richards[6], J. H. Hough[1], G. Kosugi[3], and T. Usuda[3]

[1] University of Hertfordshire, College Lane, Hatfield, Herts AL10 9AB, UK
[2] National Astronomical Observatory of Japan, 2-21-1 Osawa, Mitaka, Tokyo 181-8588, Japan
[3] Subaru Telescope, 650 North A'ohoku place, Hilo, HI 96720, USA
[4] University of Tokyo, 2-21-1 Osawa, Mitaka, Tokyo 181-8588, Japan
[5] Nagoya University Furo-cho, Chikusa-ku, Nagoya 464-8602, Japan
[6] University of Manchester, Jodrell Bank Radio obesrvatory, Macclesfield, Cheshire SK11 9DL, UK

Received 19 October 2001 / Accepted 29 September 2002

Abstract. We present J, H and K band coronagraph images of the circumstellar envelope around IRC +10216 (CW Leo) obtained with a near infrared camera, CIAO and the 8.2 m Subaru telescope. A circular occulting mask of 2″ in diameter was used to block out the light from the bright central object. The images show 2 collimated radial structures to the NNW and WNW, 2 fan-like structures to the S and NE, respectively, and 3 arc-like structures at a radius of 4 to 5 arcsec from the stellar center. We compare this intermediate size-scale structure to that seen on larger and smaller scales and find evidence for a deviation from spherically symmetric outflow beginning ∼150 years ago. Previous near infrared speckle imaging has revealed a complex clumpy structure on a scale of less than 200 mas, and it is likely that at least some of the radial features seen in our images could be due to shadowing by dust clumps close to the star.

Key words. near infrared – circumstellar envelope – individual (IRC +10216)

1. Introduction

IRC +10216 (CW Leo) is an object thought to be in transition from the asymptotic giant branch (AGB) to the proto-planetary nebula (PPN) phase. With an estimated distance of ∼120 pc (e.g. Groenewegen et al. 1998) it is one of the closest post-AGB objects and hence has an important role in our understanding of the evolution of circumstellar envelopes and the mass-loss phenomenon.

IRC +10216 is estimated to have an initial mass and a current mass of 3–5 $M_\odot$ and 0.7–0.8 $M_\odot$, respectively (Weigelt et al. 1998; Blöcker 1995 and Vassiliadis & Wood 1993), and a mass-loss rate of 2–5×10^{-5} $M_\odot\,\mathrm{yr}^{-1}$ (Loup et al. 1993). Its high mass-loss rate, at least in recent times, means that the central star is now deeply embedded in a dusty circumstellar envelope. Tamura et al. (1988), using infrared imaging-polarimetry, showed that the infrared nebulosity extends over 1′, as seen in light from the central star reflected by dust particles in the circumstellar envelope. Imaging in the V and B bands by Mauron & Huggins (1999, 2000) shows several spherical and discrete shell-like structures, extending to ∼1′ from the star. These discrete dust shells have typical thickness of 1–2″ and separations of 5–20″. Recent near-infrared speckle techniques (e.g. Weigelt et al. 1997) have produced images with a resolution better than 100 mas (e.g. Weigelt et al. 1998 and references therein for IRC +10216). Weigelt et al. (1998) and Haniff et al. (1998) obtained J, H, K and L band images of IRC +10216 that revealed 4 clumps to the north, west, south and east of the star with a separation <200 mas. These clumps may be undergoing radial expansion (Osterbart et al. 2000). Tuthill et al. (2000) discovered a dark plane which is interpreted as a prominent disk at a position angle of ∼120°. They investigated the dynamics of the dust clumps using a 7-epoch proper motion study. The dust clumps appear to escape from the star with a velocity of 11.5–25.5 mas yr^{-1} and an acceleration of 3.4 mas yr^{-2}. Using coronagraphic imaging and polarimetry, with a 5 and 7 arcsec diameter occulting mask, Kastner & Weintraub (1994) obtained images of 10″ scale structures at H and K bands. These images show a bipolar nebulosity in the N–S direction.

Send offprint requests to: K. Murakawa,
e-mail: murakawa@star.herts.ac.uk
⋆ *Present address:* Subaru Telescope, 650 North A'ohoku Place, Hilo, HI 96720, USA.

In this paper, we report near-infrared coronagraphic images using a 2″ diameter occulting mask to reveal faint structures in the inner regions around IRC +10216. The aim of our observations is to link the outflow dynamics and structures at <1″ to those on larger (>5″) scales.

2. Observations and data reduction for coronagraph imaging

Images of IRC +10216 in the J, H and K bands have been obtained with the Coronagraphic Imager with Adaptive Optics (CIAO) mounted on the 8.2 m Subaru telescope during a commissioning run on 2000 February 13 (Tamura et al. 2000). At this time adaptive optics was not available, therefore the angular resolution was limited to the natural seeing of 0.7″ in the R band. The 2″ diameter circular occulting mask was used to block out the bright central object. The mask has a transmission of about 2% which allows us to identify the stellar position. The medium resolution optics (MRM) with a plate scale of 0.0217 arcsec pix^{-1} was used. The detector is a 1024 × 1024 InSb array (ALADDIN II) manufactured by Raytheon (the former Santa Barbara Research Center).

The exposure times per frame of the J, H and K band images were 4, 2 and 2 s, respectively and 9 frames have been obtained for each band. Pre-processing involved subtraction of the dark frames from object frames and division by dome flat field frames. From these 9 object frames, we have selected frames which have a similar position of the central object and have a symmetric intensity profile for the central object. Five, three and four frames for J, H and K band, respectively, were selected and combined by centroiding on the central positions, which are assumed to be the stellar center. Even after these procedures, the position uncertainty between the star and the mask for each band is about 0.1″. HD 77281 (m_J = 7.11, m_H = 7.05, m_K = 7.03 mag) was observed as a photometric standard star. The unocculted brightness of IRC +10216 was estimated as 8.3, 4.5 and 1.2 mag in the J, H and K band, respectively.

Even using a coronagraph, diffraction patterns from the bright central object still remain in the pre-processed image. To reduce these patterns, we subtract a PSF reference image, which must include similar diffraction patterns. We confirmed the effect of PSF subtraction using K band images. A PSF reference image of HD 84780 (m_K = 4.66 mag) and a single star image of HD 106965 (m_K = 7.32 mag) were used. Each image was made by selecting frames with similar PSF shape and similar stellar position in the mask and combining them. The PSF reference image was rotated to give the same position angle of the spider pattern as that of the single star image and the flux of the PSF reference at the stellar center seen through the mask was scaled to that of the object. Then the PSF reference was subtracted from the star image (Fig. 1).

Using the same technique, the PSF reference star HD 84780 (m_J = 5.36, m_H = 4.80 mag), whose stellar position is close to the object, was subtracted from the object images. The J, H and K band images of IRC +10216, after subtraction of the PSF reference, are shown in Fig. 2. The gray scale is logarithmic. The total exposure time of the PSF reference was 20 s for all bands. While the signal-to-noise ratios (SNRs) of the PSF image in the J and H bands were better than those of the object, the exposure time for the PSF reference was comparable to that of the object in the K band, where it is 3 mag fainter than IRC +10216. This has perhaps contributed to the incomplete removal of the telescope spider pattern, visible in Fig. 2c. However, the nebula structures identified in the K band are also visible at H band so are not artifacts, although their visibility may have been improved if a greater SNR had been obtained on the PSF star in the K band.

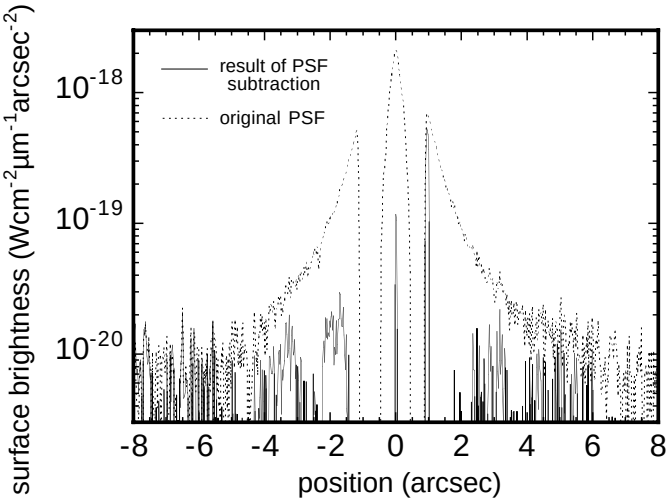

Fig. 1. Here we show the effect of PSF subtraction. The dotted curve is a radial profile of the single star HD 106965 and the solid curve is the result of PSF subtraction. Both are at K band. The PSF reference star is the single star HD 84780. The coronagraph mask is 2″ in diameter and has a transmission of 2%. The sharp feature at the center drawn as a dotted curve is due to the star image seen through the mask. The residual in the solid curve is due to the slightly different shape of the PSFs of the two stars. While the profile of HD 106965 has a strong halo component, we find that PSF subtraction removes this.

3. Morphology at a few arcsec from the star

Three discrete arc-like structures can be seen surrounding the central object, and 4 extended structures to the NNW, WNW, S and NE. The 4 extended structures consist of 2 collimated radial structures towards the NNW and NE, and 2 fan-like structures to the S and NE, respectively. The position angles (hereafter PA) of the 4 extended nebulosities to the NNW, WNW, S and NE, relative to the stellar center, are 30°, 197°, 295° and 339°, respectively. These radial structures can also be seen in the HST WFPC2 image of Skinner et al. (1998).

Figure 3 shows radial profiles of the H band image. Each profile is drawn from the center of the star at PAs of 30°, 197°, 295° and 339°, in order to intersect the 4 nebulosities to the NNW, WNW, S and NE. There can be seen bumps in each line which are due to the 3 arcs, although the SNR is low.

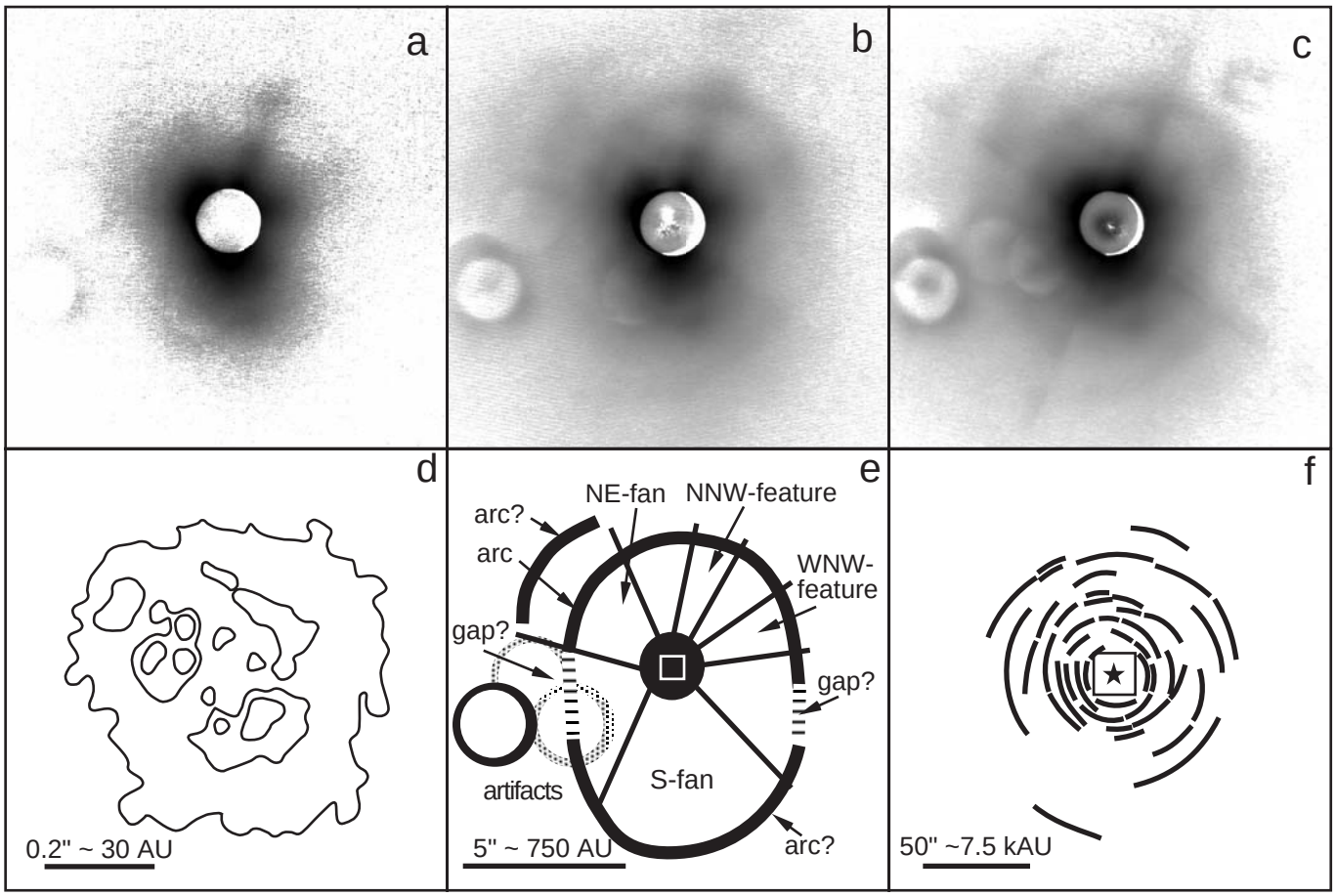

Fig. 2. The *JHK* band images, after PSF subtraction, are shown in frames **a)**–**c)**, respectively. The gray scale is logarithmic. The FOV is 640×640 pix^2 or 14×14 arcsec^2. The ring-like structures appearing on the left are ghost images caused by reflections in the CIAO optics. Four radial structures comprising 2 collimated features to the NNW and WNW and 2 fan-like structures to the NE and the S are seen. We also identify 3 arc-like structures surrounding the star; one is seen to the north, the other two are to the NE and the S. Explanatory cartoons are given in frames **d)** to **f)** which show the circumstellar environment of IRC +10216 on different scales. Frame **e)** shows, schematically, our results as described above. The black circle represents the coronagraph, and the white square is the area occupied by frame **d)**, which shows the complex clumps seen in the sub-arcsec scale images of Tuthill et al. (2000; their Fig. 1) The field of frame **e)** is represented by the square in frame **f)** which shows the larger (arcmin) scale dust shells surrounding IRC +10216 (see Fig. 8 in Mauron & Huggins 2000).

4. Discussion

IRC +10216 shows evidence of complex structure on small (<1″) to large (>10″) scales. At the largest scales (>1′) a number of discrete and spherical dust shells are seen (Mauron & Huggins 1999, 2000). Each shell has a thickness of 0.5–1″ and the inter-shell spacing is typically 5–20″. In our images, we detect arc-like structures at a radius of between 4 and 5″ from the star. We interpret these arcs as sections of the innermost AGB dust shells, expelled at the end of the AGB phase. Assuming a distance of 120 pc (Groenewegen et al. 1998) and an envelope expansion velocity of ∼15 km s^{-1} (Solomon et al. 1971), then the mass-loss event to form the last shell happened about 150 years ago. Although only sections of a complete shell are seen in our images, it appears that the arcs are not spherically symmetric, suggesting that the outflow from IRC +10216 was becoming axisymmetric by this stage. This gives the appearance of an elongated inner shell, with the axis of elongation approximately N–S.

Two prominent radial features are seen in our images. These appear to intersect the arc to the north of the star, and to continue beyond it. At the point of intersection there is a brightening, leading to a knot-like feature. This strongly suggests that these radial features are due to illumination effects caused by collimated beams of light emanating from the central region. Where these beams intersect the arc, the enhanced dust density produces the knots. It is tempting to try to correlate the positions of these radial features with the clumpy structure close to the star, as revealed by speckle imaging.

The coronagraph images of Kastner & Weintraub (1994) show a bipolar structure, with a S lobe and a NNE lobe (i.e. the lobes are not along the same axis). The same structure is visible on a smaller size scale in our images in the form of the two fan-like structures. This structure may also be compared to the HST NICMOS data (Osterbart et al. 2000) which clearly shows a bipolar nebula orientated approximately N–S with an extent of ∼2″. This smaller-scale bipolar appears to have "horn"-like features along its edges which are reminiscent of the search-light beams seen in PPNe such as AGFL 2688 (Sahai et al. 1998) and the red rectangle (Murakawa et al. in preparation, Roddier et al. 1995).

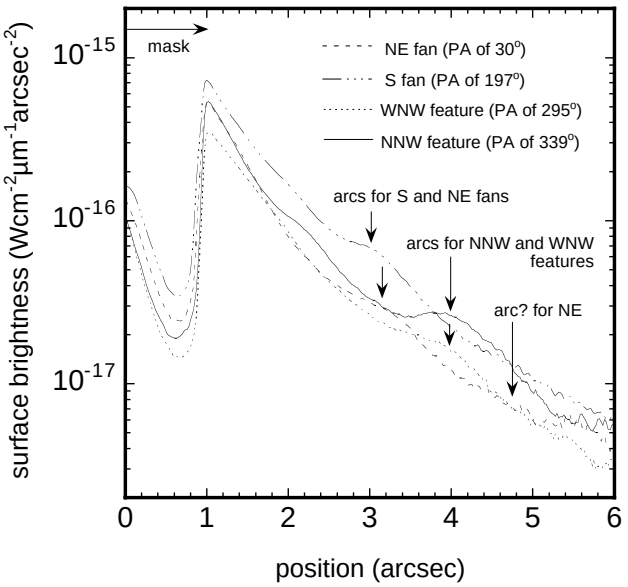

Fig. 3. Radial surface brightness profiles of the *H* band image. These cuts between the stellar center and each radial feature have PAs of 30°, 197°, 295° and 339°. There can be seen bumps at 3.2″ for the S and the NE fans, at 4.1″ for the NNW and the WNW features and at 4.7″ for the NE fan. These bumps are due to arc-like structures surrounding the star. Bumps for the S fan and the NE fan at 4.7″ are faint and cannot be seen in our images clearly.

Acknowledgements. We wish to thank the Subaru Telescope staff for the support and encouragement for our observations. K.M. acknowledges support as a PPARC funded PDRA at the University of Hertfordshire.

References

Blöcker, T. 1995, A&A, 299, 755
Cohen, M. 1979, MNRAS, 186, 837
Groenewegen, M. A. T., van der Veen, W. E. C. J., & Matthews, H. E. 1998, A&A, 338, 491
Haniff, C. A., & Buscher, D. E. 1998, A&A, 334, L5
Kastner, J. H., & Weintraub, D. A. 1994, ApJ, 434, 719
Le Bertre, T. 1997, A&A, 324, 1059
Loup, C., Forveille, T., Omont, & Paul, J. F. 1993, A&AS, 99, 391
Mauron, N., & Huggins, P. J. 1999, A&A, 349, 203
Mauron, N., & Huggins, P. J. 2000, A&A, 359, 707
Men'shchikov, A. B., Balega, Y., Blöcker, T., Osterbart, R., & Weigelt, G. 2001, A&A, 368, 497
Murakawa, K., et al., High resolution near infrared imaging of the red rectangle, in preparation
Osterbart, R., Balega, Y. Y., Blöcker, T., Men'shchikov, A. B., & Weigelt, G. 2000, A&A, 357, 169
Roddier, F., Roddier, C., Graves, J. E., & Northcott, M. J. 1995, ApJ, 443, 249
Sahai, R., Trauger, J. T., Watson, A. M., et al. 1998, ApJ, 493, 301
Skinner, C. J., Meixner, M., & Bobrowsky, M. 1998, MNRAS, 300, 29
Solomon, P., Jefferts, K. B., Penzias, A. A., & Wilson, R. W. 1971, ApJ, 163, L53
Tamura, M., Hasegawa, T., Ukita, N., et al. 1988, ApJ, 326, L17
Tamura, M., Suto, H., Itoh, Y., Ebizuka, N., et al. 2000, Proc. of SPIE
Tuthill, P. G., Monnier, J. D., Danchi, W. C., & Lopez, B. 2000, ApJ, 543, 284
Vassiladis, E., & Wood, P. R. 1993, ApJ, 413, 641
Weigelt, G. 1997, Opt. Comm., 21, 55
Weigelt, G., Balega, Y., Blöker, T., et al. 1998, A&A, 333, L51
Winters, J. M., Fleisher, A. J., Gauger, A., & Sedlmayer, E. 1994, A&A, 290, 623